# Structural reliability analysis using non-negative constraint optimization and Pade (1, 2) linearization of the limit state function

**Mehrshad Ghorbanzadeh**[a], **Peyman Homami**[b,*], **Mohsen Shahrouzi**[c]

a. Ph. D. Student, Dept. of Civil Engineering, Faculty of Engineering, Kharazmi University, Tehran 15614, Iran. Email: std_mehrshad.ghorbanzadeh@khu.ac.ir

b. Assistant Professor, Dept. of Civil Engineering, Faculty of Engineering, Kharazmi University, Tehran 15614, Iran. E-mail: *homami@khu.ac.ir*. Mobile: +989123842732 P.O. Box 15719-14911, Iran

c. Assistant Professor, Dept. of Civil Engineering, Faculty of Engineering, Kharazmi University, Tehran 15614, Iran. E-mail: shahruzi@khu.ac.ir

## Abstract

The proper performance of the first-order reliability method (FORM) is main issue in structural reliability analysis that is dependent on the accuracy, efficiency, and robustness of the employed algorithm. In this paper, a new reliability analysis framework is presented to improve the performance of the first-order reliability method. The innovation of the proposed method, which is a development on the non-negative constraint method, accounts for the estimation of the step size to implement line search formulation. The non-negative constraint method is considered to generate a positive Lagrangian function, an unconstraint optimization problem, and a search direction vector. Then, the first-order Taylor approximation of the positive constraint is applied to find the trail design point. The next step is to consider this trial design point and Pade approximation of the non-negative limit state function (constraint) for appropriately computing the step size. The efficiency and robustness of the proposed algorithm shown in various benchmark numerical examples included a comparison with other first-order reliability methods. The numerical results indicate that the proposed method functions properly to pinpoint the reliability index by fast convergence rates compared to other methods.

*Keywords*: Structural reliability analysis; Non-negative constraint method; Failure probability; Pade approximation; Optimization programming

[*] Corresponding author.
*E-mail address*: homami@khu.ac.ir (P. Homami)

## 1. Introduction

Real engineering problems include various uncertainties observed in materials, geometric properties, external loads, and other items [1–3]. Structural reliability theory provides a proper methodology for analyzing engineering structures that address structural uncertainties. This theory considers uncertainties that involve the probabilistic model to evaluate safety levels [4,5]. The main task of reliability analysis is to estimate the failure probability using a multifold integral on the failure domain. Simulation schemes and several approximation algorithms are developed because analytical multi-dimensional integration and direct numerical integration are computationally expensive [6]. Generally, the simulation methods, including Monte Carlo, importance sampling and etc., are time-consuming because thousands of samples are needed to obtain an accurate final result [7–9]. In practical engineering problems, the computational cost of the simulation methods is unacceptable because too many samples are needed to obtain an accurate result. Monte Carlo, importance sampling, etc., are some types of these methods [10,11]. Furthermore, if the value of the failure probability is too small, another problem becomes apparent. In this situation, achieving the accurate failure probability is not possible [12]. Among approximation algorithms, the first-order reliability method (FORM) is widely used and recommended in reliability analysis due to its simple and efficient algorithm.

HLRF algorithm is one of the first methods in the FORM category mainly proposed by Hasofer and Lind [13] for the random variables with the normal probability distribution and then extended by Rackwitz and Fiessler [14] for the non-normal random variables. HLRF finds the design point in standard normal space using an iterative process. The design point or the most probable point (MPP) is the point on the limit state surface with a minimum distance from the origin in the standard normal space and this closest distance is called the reliability index. Truncation, bifurcation, periodic oscillation, and chaotic behavior are instances of HLRF instability that may be observed in the limit state function with high nonlinearity. The limitations of HLRF account for the main reasons behind developing multiple methods for overcoming instability challenges. Liu and Kiureghian [15] proposed a modified HLRF (mHLRF) that used a merit function in accordance with the augmented Lagrangian scheme to estimate the step size. The iHLRF is an improvement of the HLRF proposed by Zhang and Kiureghian [16] , in which the Armijo rule is implemented to find the proper step size. They used the Lagrangian of an optimization problem to construct a simple merit function that is more efficient than mHLRF. Santosh, Saraf, Ghosh et al. developed step size estimation of mHLRF using the Goldstein rule [17]. Santos, Matioli and Beck [18] further proposed the nHLRF in which the proper step size of each iteration is selected using the Wolf rule. Yang and Cheng [19] demonstrated that the bifurcation, periodic oscillation, and chaos phenomenon of FORM are independent of the curvature value and nonlinearity of the limit state functions. Additionally, Yang proposed the stability transformation method (STM) based on chaos control theory to remove the numerical instability of HLRF [20]. The number of steps required for obtaining stable results increases if the computed step size is too small in the STM algorithm. The adaptive chaos control method proposed by Roudak, Shayanfar and Karamloo is a development of STM to reduce the number of steps required for computational iteration [21]. Meng, Yang and Zhang proposed the directional stability transformation method (DSTM) based on a directional control strategy to avoid the instability of HLRF [22]. They implemented the formulation of Lyapunov exponents for the HLRF algorithm to investigate instability phenomena. FSL investigated by Gong and Yi computes the failure probability using a finite step length parameter in the direction of gradient vector of limit state function [23]. The advanced version of this method presented by Keshtegar is the CFSL that involves the conjugate search direction introduced in the reference [24]. Keshtegar and Miri used the nonlinear conjugate gradient method and Wolf condition to propose CHLRF [25]. Three-term conjugate type of HLRF is other development of FSL presented by Keshtegar and Zhu [26]. Furthermore, Pericaro, Santos, Ribeiro et al. considered the update formula of BFGS to approximate the Hessian matrix and proposed the HLRF-BFGS algorithm [27]. Zhao, Chen and Liu speeded up the convergence rate of HLRF by applying Barzilai-Borwein gradient method [28] called BB-HLRF. This method implemented the traditional steepest descent method with specific decayed step size to achieved a proper initial point for global Barzilai-Borwein gradient algorithm.

Breitung attempted to eliminate the instability behavior of FORM using high-order Taylor expansion for the limit state surface. It is difficult and time-consuming for implicit limit state functions or a problem to include several random variables because high-order derivatives are needed for computation [29]. The second-order reliability method (SORM) is a technique of this kind that relies on the second-order Taylor expansion [16].

Roudak and Karamloo [30] developed a robust non-negative Lagrangian function (NNCM) in which the constraint of the optimization problem is changed. Indeed, NNCM introduces the square limit state function as a non-negative constraint. The first step of NNCM is directly utilizing the positive problem constraint to construct a positive Lagrangian function and a search direction vector. Then, the first-order Taylor approximation of the non-negative constraint function is employed to compute step sizes of the NNCM method that led to the efficient computation of reliability indexes in nonlinear problems.

It is important to note that the methods mentioned above implemented the first and second-order Taylor approximation of the limit state function to compute step direction and step size in the iterative process. Therefore, it is necessary to investigate the approximation method of the limit state function. Modified and multi-step Newton iterative methods with various orders of convergence are the algorithms in mathematics used to find the roots of a nonlinear equation [31–33]. Another application is the approximation of a function at a specific point. The one-step simple Newton root-finding is the method used in first-order reliability analysis. Two-step root-finding algorithms such as Double-Newton, Chun, Porta-Pták, and Pade with order (1, 2) are the methods that reduce the computational cost by increasing the convergence rate. Although these methods have high-order convergence rate, they use only the gradient of a function and are independent of higher-order derivatives [34–39]. It is noted that the search-based methods are placed in a lower class than some adaptive sampling methods such as Sequential Markov chain [40] and adaptive subset simulation [41], because these methods are invented to improve the accuracy to a high level, not to find the design point.

This study presents a combination of the non-negative constraint method and Pade approximation with order (1, 2) to define a new first-order reliability method. A new optimization problem is defined and replace with traditional optimization problem in reliability analysis. The main aim of the proposed method is to present a new relation for step size estimation that is based on Pade root finding method. Therefore, the second objective of this study is to provide a development of the non-negative constraint method for dealing with reliability problems. The difficulty of computing an appropriate penalty coefficient in iterations is eliminated by the defined optimization scheme. The proposed algorithm is particularly effective in addressing reliability problems with high nonlinearity and faster convergence than the first-order reliability method. Section two shows the step size and step direction (design point) calculation of four first-order reliability methods. Section three provides detail of the proposed algorithm for failure probability estimation. Several numerical nonlinear examples that included analytical and practical engineering problems are presented to indicate the robustness, accuracy, and efficiency of the proposed method.

## 2. First order reliability methods

There are many algorithms driven by the first-order reliability method, four of which are summarized in this section. These methods are selected to be compared with the proposed methods in numerical examples.

### 2.1 The HLRF method

HLRF investigates standard normal space to find the most probable point called MPP. MPP is a point on the limit state surface with a minimum distance from the origin. The shortest distance is the reliability index applied to evaluate failure probability. Rackwitz and Fiessler modified Hasofer and Lind method [13] by considering non-normal random variables [14]. The optimization problem used to compute the reliability index is the following optimization problem with equality constrained as shown in Eq. (1).

$$\min \ \frac{1}{2}\sqrt{U^T U} \quad \text{subjected to } G(U)=0 \tag{1}$$

Where $U$ represents the response vector of all random variables ($u_i$) in the standard normal space and $G(U)$ is the limit state function value. HLRF implements Eq. (2) to estimate the design point in each iteration.

$$U_{k+1}=\frac{\nabla^T G(U_k)U_k - G(U_k)}{\left\|\nabla G(U_k)\right\|}\nabla G(U_k) \tag{2}$$

### 2.2 The iHLRF method

The iHLRF is a development version of HLRF proposed by Zhang and Kiureghian. This algorithm used the Armijo rule to optimize the step size [16]. The iterative relation of the line search method is applied to the iHLRF as Eq. (3).

$$U_{k+1} = U_k + s_k.d_k \tag{3}$$

Where $U_k$ is the response vector that included random variable values in the standard normal space and $k$ is the step number. Parameters $s_k$ and $d_k$ are the step size value and the step direction vector, respectively. The first step of the iHLRF is to determine the step direction vector, which is defined as Eq. (4).

$$d_k = -\frac{G(U_k) - \nabla^T G(U_k) U_k}{\left\|\nabla G(U_k)\right\|} \nabla G(U_k) - U_k \tag{4}$$

The next step is to determine the step size, which is computed as Eq. (5).

$$s_k = b^j, \quad b = 0.5 \tag{5}$$

Where $j$ is an integer with an initial value equal to zero. If the convergence conditions failed to satisfy, a unit value is added to $j$. The convergence condition used for this method is defined as Eq. (6).

$$m(U_{k+1}) \le m(U_k) \tag{6}$$

In which $m$ is the merit function according to Eq. (7) and $k$ stands for iteration number.

$$m(U_m) = 0.5\left\|U_m\right\|^2 + c.\left|G(U_m)\right| \tag{7}$$

Parameter $c$ is estimated using Eq. (8) that is proposed by Zhang and Kiureghian [16].

$$c = \gamma.\frac{\left\|U_m\right\|}{\left\|\nabla G(U_m)\right\|} + \eta \;\;, \;\; \gamma = 2 \;\&\; \eta = 10 \tag{8}$$

### 2.3 The directional stability transformation method (DSTM)

On the basis of chaos control concepts, Meng, Yang and Zhan [22] proposed the directional stability transformation method to overcome the numerical instability of the HLRF method. The design point of each step is estimated using Eq. (9) in this algorithm.

$$U_{k+1} = \delta_{k+1} \frac{\omega_k}{\left\|\omega_k\right\|} \tag{9}$$

Where parameters $\delta$ and $\omega$ are calculated using Eq. (10) and Eq. (11).

$$\delta_{k+1} = -\frac{G(U_k) - \nabla^T G(U_k) U_k}{\left\|\nabla G(U_k)\right\|} \tag{10}$$

$$\omega_k = U_k + \xi C\left(f(U_k) - U_k\right) \tag{11}$$

In the above relations, $C$ is called the involuntary matrix and is considered an identity matrix. Parameter ζ is the chaos control coefficient selected in the interval [0.001, 0.1], 0.1 is suggested in the reference [22] that implemented here. The function $f(U_k)$ corresponds to Eq. (12).

$$f\left(U_k\right)=\frac{\nabla^T G\left(U_k\right)U_k-G\left(U_k\right)}{\left\|\nabla G\left(U_k\right)\right\|}\nabla G\left(U_k\right) \tag{12}$$

**2.4 The conjugate finite step length method (CFSL)**

CFSL is proposed by Keshtegar and implements the conjugate search direction on the FSL algorithm [24]. The iterative formula to find the new design point is shown in Eq. (13).

$$U_{k+1}=\frac{-d_k^T U_k-G\left(U_k\right)}{-d_k^T e_k}e_k \tag{13}$$

Where $d_k$ estimated using Eq. (14).

$$d_k=\begin{cases}-\nabla G\left(U_k\right) & k=0\\ -\nabla G\left(U_k\right)+\theta_k d_{k-1} & k\geq 1\end{cases} \tag{14}$$

Parameter $\theta_k$ can be estimated by the Eq. (15) which is conjugate descent direction.

$$\theta_k=-\frac{\left\|\nabla G\left(U_k\right)\right\|^2}{d_{k-1}^T\nabla G\left(U_k\right)} \tag{15}$$

Where the parameter $e_k$ is equal to the Eq. (16).

$$e_k=\frac{U_{k+1}^{\delta}}{\left\|U_{k+1}^{\delta}\right\|},\; U_{k+1}^{\delta}=U_k+\delta d_k \tag{16}$$

If inequality ($\|U_{k+1}-U_k\|>\|U_k-U_{k-1}\|$) is established in a step, $\delta$ is reduced to $\delta=\delta/c$ and otherwise remains unchanged. Parameter c is an adjusting coefficient considered between 1.2 and 1.5. The suggested value by Gong and Yi is 1.5 for this coefficient [23] that is implemented here.

# 3. The proposed method

The first part of this section introduces how to determine a linearization of the limit state function using the Pade approximation with order (1, 2). The second part presents the non-negative constraint method based on the first-order Taylor approximation to solve reliability problems. Then, the proposed method is introduced that is the non-negative constraint method based on the Pade approximation.

**3.1 New linearization of limit state function based on (1, 2)-Order Pade approximation**

First-order Taylor expansion is usually replaced with initial limit sate function in reliability analysis due to its simplicity and efficiency. There are many schemes used to approximate a function to avoid its initial complexity [42,43]. It is better to investigate the root-finding methods to facilitate the better understanding of the function approximation methods at a specific point [44]. Multi-step root-finding methods are more efficient than one-step methods such as simple Newton algorithm. One of the multi-steps methods is the two-step root-finding method based on Pade approximation with order (1,2) proposed by Li, Liu and Zhang in [31], which is called Pade12 in this paper. Pade12 with a fourth-order convergence avoids the operation of high-order derivatives of a function using the approximants of the second and third derivative. The one-dimensional case is shown in Eq. (17).

$$z_k = u_k - \frac{f(u_k)}{f'(u_k)}, \; u_{k+1} = u_k - \left( \frac{f(u_k) - f(z_k)}{f(u_k) - 2f(z_k)} \right)(u_k - z_k) \tag{17}$$

Where z is the predictor variable used to obtain the corrected variable of the second relation of the Eq. (17) in the next step and *k* shows the iteration number. It can be seen from Eq. (17) that only the first-order derivative of the function is applied although this root-finding method has a fourth-order convergence. The second relation of Eq. (17) can be rewritten as Eq. (18) to achieve a new approximation of the function.

$$f(u) = 0 = f'(u_k)(u_{k+1} - u_k) + \left[ \frac{f(u_k) - f(z_k)}{f(u_k) - 2f(z_k)} \right] f(u_k) \tag{18}$$

In order to extend this method to the multivariable state, it is necessary to rewrite the Eq. (18) in form $G(U)=0$, where $U$ is the vector of random variables, as shown in Eq. (19).

$$G(U) = 0 = \left[ \frac{G(U_k) - G(Z_k)}{G(U_k) - 2G(Z_k)} \right] G(U_k) + \nabla G(U_k)^T . (U_{k+1} - U_k) \tag{19}$$

Thus, a new linearization of the limit state function consisting of several variables is obtained. This new approximation merely uses the first derivative of the limit state function with respect to random variables similar to the first-order Taylor approximation. The implementation of this approximation is presented in section 3.3 to define a new step size relation in the non-negative constraint method.

### 3.2 The non-negative constraint method based on Taylor approximation

Roudak and Karamloo improved a first-order reliability method to eliminate the numerical instability of HLRF [30]. This method is the non-negative constraint method (NNCM). In the NNCM, the initial equality constraint optimization problem Eq. (1) is converted to a non-negative equality constrained optimization problem Eq. (20).

$$\min \ \frac{1}{2}\sqrt{U^T U} \quad \text{subjected to } W(U)=0 \tag{20}$$

Where the $W$ is a non-negative function equal to Eq. (21). Therefore, this method is called the non-negative constraint method.

$$W(U)=G^2(U) \tag{21}$$

The non-negative constraint is implemented to construct a non-negative Lagrangian function. This positive Lagrangian function is considered as a new unconstrained optimization problem as Eq. (22). This Equation consist of sum of the square of the objective function with the square of the constraint function multiplied by the Lagrangian coefficient based on optimization problem in Eq. (20). Then, the step direction and step size can be determined using this defined optimization problem.

$$F(U)=\frac{1}{2}U^T U+\lambda W(U) \tag{22}$$

Where $\lambda$ is the penalty coefficient. Eq (1) and (20) are the same because $G$=0 leads to $W$=0 and vice versa. Also, if Eq. (22) is considered as the unconditional optimization problem, this problem is equivalent to the equality constraint optimization problem of Eq. (20) because they have the same results. Defining a proper value of the $\lambda$ coefficient should be associated with challenges in a specific example. If this coefficient is considered too small or large, it leads to the inappropriate result in both cases. A small value for this coefficient or a light penalty reduces the effect of constraint terms in the optimization problem. On the other side, the great λ or a severe penalty coefficient may end the iteration process at a wrong point or the equality constraint cannot be satisfied. The function $F$ is always positive in Eq. (22) because all terms are positive. The first term of Eq. (22) is mathematically positive, and it is assumed that the $\lambda$ is chosen positive and large enough. The $W$ function is multiplied by the large $\lambda$; therefore, when a small value is added to the $W$ function, it causes a significant increase in the $F$ function. To minimize the non-negative $F$, $W$ has to approach zero. In other words, the optimization of the $F$ including appropriate positive $\lambda$ is guaranteed by satisfying the constraint $W$=0 or $G$=0. The $\lambda$ equal to $10^6$ is suggested by Roudak and Karamloo [30] to overcome the challenges discussed above. According to the selected value of $\lambda$, the reduction of the second term occurs faster than the first term. After determining the unconditional optimization problem in Eq. (22), the iterative process of the line search method is applied as shown in Eq. (23).

$$U_{k+1} = U_k + \alpha_k S_k \tag{23}$$

Where $S_k$ and $\alpha_k$ are the step direction and step size, respectively. The step direction is the descent direction that is selected to be the opposite of the gradient vector of the $F$ at the point $U_k$, as shown in Eq. (24).

$$S_k = -\nabla F\left(U_k\right) \tag{24}$$

Which can be rewritten in terms of $W$ as Eq. (25).

$$S_k = -\left[U_k + \lambda \nabla W\left(U_k\right)\right] \tag{25}$$

or in terms of $G$, as is shown in Eq. (26).

$$S_k = -\left[U_k + 2\lambda G\left(U_k\right)\nabla G\left(U_k\right)\right] \tag{26}$$

The next step is to determine the step size using the first-order Taylor approximation of the limit state function. This approximation is shown in Eq. (27).

$$W\left(U_{k+1}\right) \approx W\left(U_k\right) + \nabla^T W\left(U_k\right)\left(U_{k+1} - U_k\right) = 0 \tag{27}$$

Replacing Eq. (23) in the Eq. (27), one can reach Eq. (28). Not that step size is obtained using the first-order Taylor approximation. The superscript is placed to show this.

$$W\left(U_k\right) + \alpha_k^{Taylor} \nabla^T W\left(U_k\right) S_k = 0 \tag{28}$$

If Eq. (28) is solved with respect to the step size parameter, the value of the step size based on first-order Taylor approximation is obtained that is equal to Eq. (29).

$$\alpha_k^{Taylor} = \frac{W\left(U_k\right)}{\nabla^T W\left(U_k\right) S_k} = \frac{G^2\left(U_k\right)}{2G\left(U_k\right)\nabla^T G\left(U_k\right) S_k} \tag{29}$$

Determining the step size using Eq (27) is associated with the implementation of the NNCM method based on the Taylor approximation proposed by Roudak and Karamloo [30], where the value of the new design point is calculated by the line search shown in Eq. (23). In this article, this method is called NNCM-Taylor.

### 3.3 The non-negative constraint method based on Pade approximation

In this section, the main purpose is to increase the efficiency of the non-negative constraint method by providing a new relation considered to estimate step size. A new linearization of the limit state function is presented in Eq. (19) that is required for calculating the value of the limit state function at the predictor vector $Z_k$. Eq. (19) is the vectorized of the Eq. (17). In the first relation of Eq (17), it is observed that the

$Z_k$ vector is obtained using the first-order Taylor approximation in the root-finding method. This vector is replaced with the output obtained by the non-negative constraint method based on the first-order Taylor approximation in the reliability analysis. In other words, the design point estimated for the non-negative constraint method based on the Taylor approximation is considered as the predictor vector or trail design point ($Z_k$). Then, the step size is calculated in the non-negative constraint method based on the Pade approximation. Eq. (30) shows the proposed relation of the predictor vector $Z_k$.

$$Z_k = U_k + \alpha_k^{Taylor} S_k \tag{30}$$

If the $Z_k$ is available, the value of $G(Z_k)$ or $W(Z_k)$ is estimated. At this point, the non-negative $W$ function can be rewritten using the Pade approximation as Eq. (31).

$$W(U_{k+1}) \approx 0 = \left[\frac{W(U_k) - W(Z_k)}{W(U_k) - 2W(Z_k)}\right] W(U_k) + \nabla W(U_k)^T (U_{k+1} - U_k) \tag{31}$$

According to the non-negative constraint method based on Taylor approximation (NNCM-Taylor), the Eq. (23) can be replaced in the Eq (31), $U_{k+1}$-$U_k = \alpha_k S_k$, to obtain Eq. (32). Note that at this level, the step size is based on Pade approximation, $\alpha_k = \alpha_k^{Pade}$. The superscript of step size parameter is placed to indicate this in Eq. (32).

$$\left[\frac{W(U_k) - W(Z_k)}{W(U_k) - 2W(Z_k)}\right] W(U_k) + \alpha_k^{Pade} \nabla W(U_k)^T S_k = 0 \tag{32}$$

The Eq. (32) can also be defined in terms of $G(U_k)$ that is shown in Eq. (33).

$$\left[\frac{G^2(U_k) - G^2(Z_k)}{G^2(U_k) - 2G^2(Z_k)}\right] G^2(U_k) + 2G(U_k)\alpha_k^{Pade} \nabla G(U_k)^T S_k = 0 \tag{33}$$

Therefore, the step size based on the Pade approximation with order (1, 2) is expressed as Eq. (34).

$$\alpha_k^{Pade} = \frac{-\left[\frac{W(U_k) - W(Z_k)}{W(U_k) - 2W(Z_k)}\right] W(U_k)}{\nabla W(U_k)^T S_k} \tag{34}$$

or in terms of $G(U_k)$, as is shown in Eq. (35).

$$\alpha_k^{Pade} = \frac{-\left[\frac{G^2(U_k) - G^2(Z_k)}{G^2(U_k) - 2G^2(Z_k)}\right] G^2(U_k)}{2G(U_k)\nabla G(U_k)^T S_k} \tag{35}$$

It is observed that the step direction is obtained by Eq (25) or (26), and the step size is computed by Eq (34) or (35) based on the Pade approximation. Then, the new design point can be estimated using Eq (23) by replacing step direction and step size value. This process continues until convergence conditions are satisfied. This iterative process of updating MMP is called NNCM-Pade, the method proposed in this paper. The main feature of NNCM-Pade includes taking fewer steps compared to NNCM-Taylor to find the design point. The faster convergence rate of the proposed method is confirmed by observing the results in section four. Another point is that although both non-negative constraint methods have the same step direction, the NNCM-Pade algorithm uses the computed step direction of the NNCM-Taylor algorithm to come up with a more appropriate result in each step. In other words, the difference between the two methods refers to the step size calculation. Table 1 shows the computational steps required for implementing the proposed method. If the correlated non-normal random variables are considered for a problem, the Nataf transformation method is implemented to find the failure probability.

**Table 1.**

## 4. Numerical examples

Several numerical examples have been taken from the literature in order to examine the functionality of the proposed method. The tables and diagrams are employed to compare the results. In each example, the final results of the proposed method and five reliability algorithms including HLRF, iHLRF, DSTM, CFSL, and NNCM-Taylor are compared. The requirements for using these methods were listed in the previous sections. The failure probability of Monte Carlo sampling (MCS) and the number of generated samples are presented in the tables to provide precise results. In order to ensure the integrity, when $|\beta_k-\beta_{k+1}|<10^6$ is met, the convergence of an algorithm is accepted. It should be noted that in all reliability algorithms, finite difference method is employed for numerically estimating gradient vector. In addition, the examples can be solved in BI software which is a computer program for doing reliability analysis that is developed by the authors of this article and can be downloaded from *www.betaindexsoftware.com*, where the examples can be modeled.

### 4.1 Example 1: a highly nonlinear quartic polynomial LSF

The first example considers the following highly nonlinear and quadratic polynomial performance function [45,46], Eq. (36).

$$G(X) = X_1 - 1.7X_2 + 1.5(X_1 + 1.7X_2)^2 + 5 \quad (36)$$

Where both $X_1$ and $X_2$ have normal probability distribution with means and standard deviations of 0 and 1, respectively. Table 2 lists information including the number of iterations, value of reliability index, probability of failure, number of limit state function evaluation, and the term $|\beta-\beta_{MCS}|$.

**Table 2.**

Fig 1 shows the convergence histories of the algorithms. As can be seen in Table 2 and Fig 1, the methods including HLRF, DSTM, and CFSL fail to converge which is a sign of high nonlinearity associated with this problem. Other methods represent the stable results of reliability index. The fast convergence belongs to NNCM-Pade and NNCM-Taylor with 12 and 21 steps, respectively. The response of iHLRF is accurate, but the function evaluation of iHLRF is inefficient (1295 calls). The last row of Table 3 pertains to MCS results obtained using $10^6$ simulations. As can be observed, the terms $|\beta-\beta_{MCS}|$ of the methods are approximately 0.46 and close to each other. The corresponding $\beta = 2.87$ is the best result expected from a first-order method. In other words, the difference between the final results of the Monte Carlo simulation and other methods is due to following the methods that rely on the first-order approximation. Thus, the competitive feature of the method is associated with the number of required steps to resolve the problem.

**Fig 1.**

### 4.2 Example 2: a highly nonlinear quadratic polynomial LSF

The second example considers the following fourth-order polynomial performance function including three independent random variables with non-normal probability distributions [47], Eq. (37).

$$G(X) = X_1^4 + X_2^2 - 50 \quad (37)$$

Table 3 shows statistical properties of random variables.

**Table 3.**

The final results are listed for different reliability algorithms in Table 4. As can be seen, except for the HLRF method, other methods have reached a stable reliability index. The responses to CFSL and DSTM methods are accurate and these algorithms have the same number of iterations and function evaluations. NNCM-Pade and NNCM-Taylor require the fewest iterations (12 and 23). Although iHLRF obtains the proper reliability index, the computation cost (515 function evaluations) is too high. The terms $|\beta-\beta_{MCS}|$ are approximately 0.30. The corresponding $\beta$= 3.56 is the best response expected from a first-order method.

**Table 4.**

The convergence histories are shown in Fig 2. The non-convergence of HLRF and convergence of other methods are demonstrated. The soft convergence of NNCM-Taylor and NNCM-Pade as well as the fluctuation convergence of iHLRF, CFSL, and DSTM are shown in the Fig 2. The fluctuation of the DSTM is less than CFSL and related to the last iterations.

**Fig 2.**

### 4.3 Example 3: highly nonlinear quadratic polynomial LSF with three variables

Eq. (38) presents a limit state function for Example 3 [48].

$$G\left(X\right)=X_3+\left(\frac{X_1-1.1}{1.5}\right)^2-\left(\frac{X_2-0.2}{3}\right)^2+3.6 \qquad (38)$$

All random variables are independent standard normal random variables. According to Table 5, the HLRF fails to converge. NNCM-Pade features the best performance with 11 steps and 55 function evaluations. Reliability index of MCS is obtained using $10^6$ samples. NNCM-Taylor and CFSL show proper efficiencies by 19 and 16 iterations, respectively. The corresponding $\beta$= 3.70 is the best response expected from a first-order method. The terms $|\beta-\beta_{MCS}|$ are about 0.018.

**Table 5.**

Fig 3 shows the convergence histories. The chaotic behavior of HLRF can be seen in this Fig. However, other algorithms converge with different efficiencies. The HLRF method starts to oscillate between 3 points after the seventh step and is not able to converge.

The difference between the NNCM-Taylor and NNCM-Pade methods is related to the step size value. The larger step size of the NNCM-Pade is the key point and the results of the fast convergence of the proposed method are compared to NNCM-Taylor. The DSTM method is associated with oscillations in the initial steps, which gradually decreases when the convergence process is achieved. iHLRF which utilizes Armijo rule shows less fluctuation compared to CFSL which is implemented by finite step length.

**Fig 3.**

### 4.4 Example 4: cantilever column

In this example, a cantilever column is investigated as shown in Fig 4.

**Fig 4.**

The length, modulus of elasticity, and moment of inertia are L, E, and I, respectively. The horizontal and vertical loads H and P are applied to the end of the column. The column is connected to the base by a rotational spring with stiffness *b* [30]. The statics of the random variables is presented in Table 6.

**Table 6.**

The horizontal displacement is used to define the limit state function as Eq. (39).

$$G(X) = 10 - \Delta \tag{39}$$

Where Δ is the horizontal displacement shown by Eq. (40) under the applied loads.

$$\Delta = \frac{H}{EI\left(a\right)^{\frac{3}{2}}} \times \left[ \tan\left(L\sqrt{a}\right) - L\sqrt{a} + \frac{b^2\left\{1-\sqrt{c\tan^2\left(L\sqrt{a}\right)}\right\}^2}{4HEI\left(L\sqrt{a}\right)} \right],\ a = \frac{P}{EI}\ ,\ c = \frac{4HEI}{b^2} \tag{40}$$

Table 7 compares the results of different methods. The Monte Carlo simulation is done with $2\times10^6$ simulations to obtain the reliability index of 4.0253. HLRF stopped functioning after the first iteration and failed to converge. The iHLRF method that uses the Armijo rule and step size reduction process has fast convergence, but 195 function evaluations are inefficient. NNCM-Pade and DSTM yield the final results by 10 and 11 steps (80 and 77 function evaluations). Then, NNCM-Taylor and CFSL have the close performance to each other.

**Table 7.**

The convergence histories are shown in Fig 5. In terms of solution steps, there are two categories of algorithms. HLRF, DSTM, and CFSL are the same in the first step, but HLRF fails to continue iteration because it has reached a critical point. However, DSTM and CFSL did not stop at this critical point. NNCM-Pade, NNCM-Taylor, and iHLRF are placed in the second category and move along the same route. This problem is solved by Generalized HL-RF, proposed by [49] leading to $\beta$ = 4.1108. The corresponding $\beta = 4.11$ is the best response expected from a first-order method. The terms $|\beta\text{-}\beta_{MCS}|$ are about 0.09.

**Fig 5.**

### 4.5 Example 5: cantilever tube

In this example, a cantilever tube beam is considered [30]. The forces $F_1$, $F_2$, P, and the torsion moment T are applied to this beam. Eq. (41) shows the limit state function.

$$G(X) = S_y - \sqrt{\sigma_x^2 + 3\tau_{zx}^2} \tag{41}$$

Where $S_y$ is the strength. The stresses $\sigma_x$ and $\tau_{zx}$ are given by Eq. (42).

$$\sigma_x = \frac{P + F_1 \sin(\theta_1) + F_2 \sin(\theta_2)}{A} + \frac{Md}{2I} \ , \ \tau_{zx} = \frac{Td}{4I} \tag{42}$$

Where the parameters are defined as Eq. (43).

$$M = F_1 L_1 \cos(\theta_1) + F_2 L_2 \cos(\theta_2) \ , A = \frac{\pi}{4}\left[d^2 - (d-2t)^2\right] , \ I = \frac{\pi}{64}\left[d^4 - (d-2t)^4\right] \tag{43}$$

Table 8 shows the properties of the random variables.

**Table 8.**

Cross section, dimensions, axes, and applied load states of the cantilever tube beam are depicted in Fig 6.

**Fig 6.**

The results of this problem are presented in Table 9. Similar to previous examples, the NNCM-Pade has the minimum number of iterations to achieve a stable response compared to other methods. NNCM-Taylor and DSTM also yield proper results. Compared to CFSL, despite the proximity of iteration number, iHLRF requires a higher number of function evaluation which is not desirable.

**Table 9.**

Fig 7 shows convergence histories. HLRF oscillates between two wrong points with the periodic responses. How different methods converge is evident in this Fig. Note that the low-level change between iHLRF diagram fractures is due to the step reduction effect. In addition, the slow convergence in the CFSL method is related to the effect of the adjusting coefficient (c) in this method. The other case in Fig 7 represents the two NNCM-Pade and NNCM-Taylor algorithms with similar formulations that yielded relatively similar results.

**Fig 7.**

### 4.6 Example 6: a space truss structure

An implicit limit state function of a space truss structure is presented in this example. There are 24 truss elements and 7 concentrated loads. $P_1$ is applied to the central node, and $\theta$ determines the direction of $P_1$ on the X-Z plane. The other loads ($P_2$-$P_7$) are inserted into nodes in the Z-direction without inclination. $A_i$ is the cross-sectional area of element i. $E_1$, $E_2$, and $E_3$ are the modulus of element elasticity 1–6, 7–12, and 13-24, respectively. The implicit limit state function is specified by the maximum vertical displacement (Δ) of the central node as Eq. (44) [30].

$$G(X) = 0.01 - \Delta \tag{44}$$

The statics of the random variables are presented in Table 10.

**Table 10.**

Fig 8 shows the space truss structure including the number of elements, dimensions, axes, and applied load states.

**Fig 8.**

Table 11 shows the results of different methods. The reliability index result of the Monte Carlo simulation is obtained using $10^6$ samples. The divergence is demonstrated in HLRF and iHLRF due to the high nonlinearity of the problem. Although CFSL provides the final response, the number of steps is too high. DSTM and NNCM-Taylor show appropriate performance, but NNCM-Pade has the best performance. The failure probability of the NNCM-Pade algorithm is estimated with 13 iterations which is the sign of a fast convergence rate. Except for NNCM-Pade, the results of other methods demonstrated in Table 11 can be derived from the literature [30].

**Table 11.**

The convergence histories are shown in Fig 9.

**Fig 9.**

## 5. Discussion

In this paper, the performance of the proposed method (NNCM-Pade), which integrates non-negative constraint method (NNCM) and Pade approximation with order (1,2), investigated using the five nonlinear examples in ensuring both effectiveness and convergence aspects. The calculated reliability index, the number of iterations, and the function evaluations are the main items used for comparisons. The results of other reliability methods, including HLRF, iHLRF, DSTM, CFSL, and NNCM-Taylor are presented for comparison. Further, the output of the Monte Carlo simulation is evaluated as the accurate output of each example.

NNCM-Pade and NNCM-Taylor are the methods that successfully cover all examples and estimate the failure probability. However, the NNCM-Pade is more efficient and robust than NNCM-Taylor. It occurs because the proposed method includes all the tools of the NNCM-Taylor, an additional step in determining the step size. Therefore, the computational effort is decreased by the proposed method. The second term of the Lagrange function, including the multiplication of the $\lambda$ coefficient and the $W$, is a positive value that the NNCM methods have to make it zero because the minimization of the Lagrange function depends on it. Thus, achieving the limit state function close to zero is immediately observed in NNCM methods. Then, NNCM-Pade needs less iteration to compute the reliability index against NNCM-Taylor because it uses the Pade approximation that leads to proper step size estimation.

The accuracy of the proposed method is obtained by comparing its final response with other methods and the Monte Carlo method, where the proposed method is accurate.

Accuracy, robustness, and efficiency are intended to control the methods mentioned in this article. The accuracy of the proposed method is obtained by comparing its final response with other methods and the Monte Carlo simulation, where the proposed method is accurate. The number of iterations and function evaluations could be considered as a criterion for evaluating the efficiency of the proposed method. The stable and non-oscillating final response is also a sign of robustness, which is a relative quantity. Based on these three criteria, the proposed method performs acceptably in the presented examples.

The success of the NNCM-Pade in the nonlinear problems proves the robustness, accuracy, and fast convergence of this method. A few required steps are the most significant competitive features of the proposed method observed in all examples of this paper. This feature is substantial because each computational iteration in the implicit reliability problem, involving a complex and large-scale finite element model, imposes a high computational cost on reliability analysis. As shown in tables, the sampling methods such as Monte Carlo simulation require thousands of samples. Therefore, the NNCM-Pade is an appropriate choice for numerical and practical engineering problems.

## 6. Conclusions

A robust and efficient method based on the non-negative constraint method and Pade approximation for analyzing structural reliability is presented in this article. The proposed algorithm called NNCM-Pade can eliminate some of the instability issues of the HLRF algorithm and it use a new step size formulation to increase convergence ratio. The stability of the proposed method is obtained from the non-negative constraint method using the descent step direction estimation and trail design point evaluation. Then, the Pade approximation of the limit state function is considered to achieve the fast convergence by the appropriate step size calculation. The main advantage of this algorithm is that it is really simple and reduces computational efforts because the optimization programing implemented in this method is different from other algorithms. Moreover, it is a capable tool for finding the design point in reliability analysis. It is noted that when the sampling method is used to obtain a highly accurate result of the reliability analysis, the proposed method can be used to determine the better starting point.

Through the application of several numerical and practical engineering examples, it is indicated that NNCM-Pade is a robust, accurate, and efficient algorithm that could be implement in reliability analysis.

## 7. Acknowledgment

This research did not receive any specific grant from funding agencies in the public, commercial, or not-for-profit sectors.

## 8. References

1. Yang, S., Wang, J., and Yang, H., "Evidence Theory based Uncertainty Design Optimization for Planetary Gearbox in Wind Turbine", *J. Adv. Appl. Comput. Math.*, **9**, pp. 86–102 (2022).

2. Debiao, M., Shiyuan, Y., Tao, L., Jiapeng, W., Hengfei, Y., and Zhiyuan, L., "RBMDO Using Gaussian MixtureModel-Based Second-OrderMean-Value Saddlepoint Approximation", *C. - Comput. Model. Eng. Sci.*, **132**(2), pp. 553–568 (2022).

3. Meng, D., Yang, S., He, C., Wang, H., Lv, Z., Guo, Y., and Nie, P., “Multidisciplinary design optimization of engineering systems under uncertainty: a review”, *Int. J. Struct. Integr.*, **13**(4), pp. 565–593 (2022).

4. Zhou, M., Shadabfar, M., Xue, Y., Zhang, Y., and Huang, H., “Probabilistic Analysis of Tunnel Roof Deflection under Sequential Excavation Using ANN-Based Monte Carlo Simulation and Simplified Reliability Approach”, *ASCE-ASME J. Risk Uncertain. Eng. Syst. Part A Civ. Eng.*, **7**(4), p. 04021043 (2021).

5. Meng, D., Lv, Z., Yang, S., Wang, H., Xie, T., and Wang, Z., “A time-varying mechanical structure reliability analysis method based on performance degradation”, *Structures*, **34**, pp. 3247–3256 (2021).

6. Yu, X., He, Z., and Ning, C.-L., “Advanced Dimension-Adaptive Sparse Grid Integration Method for Structural Reliability Analysis”, *ASCE-ASME J. Risk Uncertain. Eng. Syst. Part A Civ. Eng.*, **7**(3), p. 04021031 (2021).

7. Meng, D., Yang, S., Jesus, A. M. P. de, and Zhu, S.-P., “A novel Kriging-model-assisted reliability-based multidisciplinary design optimization strategy and its application in the offshore wind turbine tower”, *Renew. Energy*, **203**, pp. 407–420 (2023).

8. Yoshida, I. and Shuku, T., “Bayesian Updating of Model Parameters by Iterative Particle Filter with Importance Sampling”, *ASCE-ASME J. Risk Uncertain. Eng. Syst. Part A Civ. Eng.*, **6**(2), p. 04020007 (2020).

9. Jafari-Asl, J., Ohadi, S., Ben Seghier, M. E. A., and Trung, N.-T., “Accurate Structural Reliability Analysis Using an Improved Line-Sampling-Method-Based Slime Mold Algorithm”, *ASCE-ASME J. Risk Uncertain. Eng. Syst. Part A Civ. Eng.*, **7**(2), p. 04021015 (2021).

10. Bjerager, P., “Probability Integration by Directional Simulation”, *J. Eng. Mech.*, **114**(8), pp. 1285–1302 (1988).

11. Engelund, S. and Rackwitz, R., “A benchmark study on importance sampling techniques in structural reliability”, *Struct. Saf.*, **12**(4), pp. 255–276 (1993).

12. Bucher, C. G., “Adaptive sampling — an iterative fast Monte Carlo procedure”, *Struct. Saf.*, **5**(2), pp. 119–126 (1988).

13. Hasofer, A. M. and Lind, N. C., “Exact and Invariant Second-Moment Code Format.”, *ASCE J Eng Mech Div*, **100**(EM1), pp. 111–121 (1974).

14. Rackwitz, R. and Flessler, B., “Structural reliability under combined random load sequences”, *Comput. Struct.*, **9**(5), pp. 489–494 (1978).

15. Liu, P. L. and Der Kiureghian, A., “Optimization algorithms for structural reliability”, *Struct. Saf.*, **9**(3), pp. 161–177 (1991).

16. Zhang, Y. and Kiureghian, A., “Two Improved Algorithms for Reliability Analysis”, In *Reliability and Optimization of Structural Systems*, Springer US, Boston, MA, pp. 297–304 (1995).

17. Santosh, T. V., Saraf, R. K., Ghosh, A. K., and Kushwaha, H. S., “Optimum step length selection rule in modified HL-RF method for structural reliability”, *Int. J. Press. Vessel. Pip.*, **83**(10), pp. 742–748 (2006).

18. Santos, S. R., Matioli, L. C., and Beck, A. T., “New optimization algorithms for structural reliability analysis”, *C. -*

*Comput. Model. Eng. Sci.*, **83**(1), pp. 23–55 (2012).
19. Yang, D., Li, G., and Cheng, G., "Convergence analysis of first order reliability method using chaos theory", *Comput. Struct.*, **84**(8–9), pp. 563–571 (2006).
20. Yang, D., "Chaos control for numerical instability of first order reliability method", *Commun. Nonlinear Sci. Numer. Simul.*, **15**(10), pp. 3131–3141 (2010).
21. Roudak, M. A., Shayanfar, M. A., and Karamloo, M., "Improvement in first-order reliability method using an adaptive chaos control factor", *Structures*, **16**, pp. 150–156 (2018).
22. Meng, Z., Li, G., Yang, D., and Zhan, L., "A new directional stability transformation method of chaos control for first order reliability analysis", *Struct. Multidiscip. Optim.*, **55**(2), pp. 601–612 (2017).
23. Gong, J.-X. X. and Yi, P., "A robust iterative algorithm for structural reliability analysis", *Struct. Multidiscip. Optim.*, **43**(4), pp. 519–527 (2011).
24. Keshtegar, B., "A hybrid conjugate finite-step length method for robust and efficient reliability analysis", *Appl. Math. Model.*, **45**, pp. 226–237 (2017).
25. Keshtegar, B. and Miri, M., "Introducing conjugate gradient optimization for modified HL-RF method", *Eng. Comput. (Swansea, Wales)*, **31**(4), pp. 775–790 (2014).
26. Keshtegar, B. and Zhu, S.-P., "Three-term conjugate approach for structural reliability analysis", *Appl. Math. Model.*, **76**, pp. 428–442 (2019).
27. Periçaro, G. A., Santos, S. R., Ribeiro, A. A., and Matioli, L. C., "HLRF–BFGS optimization algorithm for structural reliability", *Appl. Math. Model.*, **39**(7), pp. 2025–2035 (2015).
28. Zhao, W., Chen, Y., and Liu, J., "An effective first order reliability method based on Barzilai–Borwein step", *Appl. Math. Model.*, **77**, pp. 1545–1563 (2020).
29. Breitung, K. W., *Asymptotic Approximations for Probability Integrals*, Lecture Notes in Mathematics, Springer Berlin Heidelberg, Berlin, Heidelberg (1994).
30. Roudak, M. A. and Karamloo, M., "Establishment of non-negative constraint method as a robust and efficient first-order reliability method", *Appl. Math. Model.*, **68**, pp. 281–305 (2019).
31. Li, S., Liu, X., and Zhang, X., "A Few Iterative Methods by Using [1,n]-Order Padé Approximation of Function and the Improvements", *Mathematics*, **7**(1), p. 55 (2019).
32. Ali, F., Aslam, W., Ali, K., Anwar, M. A., and Nadeem, A., "New Family of Iterative Methods for Solving Nonlinear Models", *Discret. Dyn. Nat. Soc.*, **2018**, pp. 1–12 (2018).
33. Wang, X., Qin, Y., Qian, W., Zhang, S., and Fan, X., "A family of Newton type iterative methods for solving nonlinear equations", *Algorithms*, **8**(3), pp. 786–798 (2015).
34. Young, D. M., Traub, J. F., Young, D. M., Traub, J. F., Young, D. M., and Traub, J. F., "Iterative Methods for the

Solution of Equations.", *Am. Math. Mon.*, **74**(3), p. 346 (1967).

35. Chun, C., "Some fourth-order iterative methods for solving nonlinear equations", *Appl. Math. Comput.*, **195**(2), pp. 454–459 (2008).

36. Potra, F. and Pták, V., *Nondiscrete Induction and Iterative Processes. Number*, Pitman Advanced Pub. Program, Boston (1984).

37. Sharma, J. R., "A composite third order Newton-Steffensen method for solving nonlinear equations", *Appl. Math. Comput.*, **169**(1), pp. 242–246 (2005).

38. Argyros, I. K. and Hilout, S., "On the semilocal convergence of damped Newton's method", *Appl. Math. Comput.*, **219**(5), pp. 2808–2824 (2012).

39. Xiaojian, Z., "Modified Chebyshev–Halley methods free from second derivative", *Appl. Math. Comput.*, **203**(2), pp. 824–827 (2008).

40. Yera, Y. G., Lillo, R. E., Nielsen, B. F., Ramírez-Cobo, P., and Ruggeri, F., "A bivariate two-state Markov modulated Poisson process for failure modeling", *Reliab. Eng. Syst. Saf.*, **208**, p. 107318 (2021).

41. Zhao, Y. and Wang, Z., "Subset simulation with adaptable intermediate failure probability for robust reliability analysis: an unsupervised learning-based approach", *Struct. Multidiscip. Optim.*, **65**(6), p. 172 (2022).

42. Masjed-Jamei, M., Moalemi, Z., Area, I., and Nieto, J. J., "A new type of Taylor series expansion", *J. Inequalities Appl.*, **2018**(1), p. 116 (2018).

43. Chen, H., "A power series expansion and its applications", *Int. J. Math. Educ. Sci. Technol.*, **37**(3), pp. 362–368 (2006).

44. *Iterative Methods for Solving Nonlinear Equations and Systems*, MDPI (2020).

45. Jiang, C., Han, S., Ji, M., and Han, X., "A new method to solve the structural reliability index based on homotopy analysis", *Acta Mech.*, **226**(4), pp. 1067–1083 (2015).

46. Yang, M., Zhang, D., and Han, X., "New efficient and robust method for structural reliability analysis and its application in reliability-based design optimization", *Comput. Methods Appl. Mech. Eng.*, **366**, p. 113018 (2020).

47. Keshtegar, B., "Chaotic conjugate stability transformation method for structural reliability analysis", *Comput. Methods Appl. Mech. Eng.*, **310**, pp. 866–885 (2016).

48. Gong, J., Yi, P., and Zhao, N., "Non-Gradient–Based Algorithm for Structural Reliability Analysis", *J. Eng. Mech.*, **140**(6), p. 04014029 (2014).

49. Roudak, M. A., Shayanfar, M. A., Barkhordari, M. A., and Karamloo, M., "A robust approximation method for nonlinear cases of structural reliability analysis", *Int. J. Mech. Sci.*, **133**, pp. 11–20 (2017).

**List of Tables**



**List of Figures**

**Fig. 8.** Space truss of Example 6

**Fig. 9.** Iteration history for Example 6

**Table 1.** The algorithm of the non-negative constraint method based on Pade approximation

1. Set $k$ = 0, $\lambda = 10^6$
2. Select a start point, $U_k$
3. Evaluate step direction vector $S_k$ from Eq. (23) or (24) at point $U_k$
4. Evaluate step size value based on Taylor approximation from first or second term of Eq. (29)
5. Evaluate predictor vector $Z_k$ from Eq. (30)
6. Evaluate value of limit state function at point $Z_k$
7. Evaluate step size value based on Pade approximation from Eq. (34)
8. Locate design point of next iteration $U_{k+1}$ by Eq. (23) in which step size of step 7 is implemented
9. Evaluate $\beta_{k+1} = ||U_{k+1}||$
10. If $|\beta_{k+1} - \beta_k| < 10^{-4}$:
    - k = k+1,
    - Go to step 3,
    
    else:
    - Design point = $U_{k+1}$,
    - Reliability index = $\beta_{k+1}$,
    - Probability of failure = $P_f = \Phi(-\beta_{k+1})$

**Table 2.** Results of various methods for Example 1

| Method | $\beta$ | $P_f$ | Iterations | G-Evaluations | $\lvert\beta-\beta_{MCS}\rvert$ |
|---|---|---|---|---|---|
| *HLRF* | Not convergence | ------------- | ---- | ---- | ------- |
| *iHLRF* | 2.8749 | 0.002020 | 100 | 1295 | 0.4646 |
| *DSTM* | Not convergence | ------------- | ---- | ---- | ------- |
| *CFSL* | Not convergence | ------------- | ---- | ---- | ------- |
| *NNCM-Taylor* | 2.8787 | 0.001996 | 21 | 66 | 0.4608 |
| *NNCM-Pade* | 2.8787 | 0.001996 | 12 | 52 | 0.4608 |
| *MCS* | 3.3395 | 0.000419 | ---- | $10^6$ | 0.0000 |

**Table 3.** Probability distribution of random variable for Example 2

| Variable | Distribution | Mean | Standard deviation |
|---|---|---|---|
| $X_1$ | Lognormal | 5.0 | 1.0 |
| $X_3$ | Gumbel | 10.0 | 10.0 |

**Table 4.** Results of various methods for Example 2

| Method | $\beta$ | $P_f$ | Iterations | G-Evaluations | $\lvert\beta-\beta_{MCS}\rvert$ |
|---|---|---|---|---|---|
| *HLRF* | Not convergence | ------------- | ---- | ---- | ------- |
| *iHLRF* | 3.2593 | 0.000553 | 39 | 515 | 0.3019 |
| *DSTM* | 3.2593 | 0.000553 | 31 | 93 | 0.3019 |
| *CFSL* | 3.2593 | 0.000553 | 32 | 96 | 0.3019 |
| *NNCM-Taylor* | 3.2593 | 0.000553 | 23 | 69 | 0.3019 |
| *NNCM-Pade* | 3.2593 | 0.000553 | 12 | 48 | 0.3019 |
| *MCS* | 3.5612 | 0.000184 | ---- | $10^6$ | 0.0000 |

**Table 5.** Results of various methods for Example 3

| Method | $\beta$ | $P_f$ | Iterations | G-Evaluations | $\lvert\beta-\beta_{MCS}\rvert$ |
|---|---|---|---|---|---|
| *HLRF* | Not convergence | ------------- | ---- | ---- | ------- |
| *iHLRF* | 3.7050 | 0.000105 | 36 | 517 | 0.0186 |
| *DSTM* | 3.7050 | 0.000105 | 84 | 336 | 0.0186 |
| *CFSL* | 3.7050 | 0.000105 | 16 | 64 | 0.0186 |
| *NNCM-Taylor* | 3.7050 | 0.000105 | 19 | 76 | 0.0186 |
| *NNCM-Pade* | 3.7050 | 0.000105 | 11 | 55 | 0.0186 |
| *MCS* | 3.7236 | 0.000098 | ---- | $10^6$ | 0.0000 |

**Table 6.** Probability distribution of random variable for Example 4

| Variable | Distribution | Mean | Standard deviation |
|---|---|---|---|
| $P$ (kips) | Lognormal | 10 | 3 |
| $H$ (kips) | Lognormal | 5.8 | 1.16 |
| $E$ (ksi) | Lognormal | $2.9\times10^4$ | $0.58\times10^4$ |
| $L$ (in) | Lognormal | 144 | 7.2 |
| $I$ ($in^4$) | Lognormal | 88.6 | 8.86 |
| $b$ (kips.in/rad) | Lognormal | $3\times10^4$ | $0.3\times10^4$ |

**Table 7.** Results of various methods for Example 4

| Method | $\beta$ | $P_f$ | Iterations | G-Evaluations | $\lvert\beta-\beta_{MCS}\rvert$ |
|---|---|---|---|---|---|
| *HLRF* | Not convergence | ------------- | ---- | ---- | ------- |
| *iHLRF* | 4.1108 | $1.9712\times10^{-5}$ | 12 | 195 | 0.0854 |
| *DSTM* | 4.1108 | $1.9712\times10^{-5}$ | 11 | 77 | 0.0855 |
| *CFSL* | 4.1108 | $1.9712\times10^{-5}$ | 23 | 161 | 0.0855 |
| *NNCM-Taylor* | 4.1108 | $1.9712\times10^{-5}$ | 17 | 119 | 0.0912 |
| *NNCM-Pade* | 4.1108 | $1.9712\times10^{-5}$ | 10 | 80 | 0.0859 |
| *MCS* | 4.0253 | $2.8451\times10^{-5}$ | ---- | $2\times10^6$ | 0.0000 |

**Table 8.** Probability distribution of random variable for Example 5

| Variable | Distribution | Mean | Standard deviation |
|---|---|---|---|
| $t$ (mm) | Normal | 5 | 0.1 |
| $d$ (mm) | Normal | 42 | 0.5 |
| $L_1$ (mm) | Normal | 119.75 | 11.975 |
| $L_2$ (mm) | Normal | 59.75 | 5.975 |
| $F_1$ (N) | Lognormal | 3000 | 300 |
| $F_2$ (N) | Lognormal | 3000 | 300 |
| $P$ (N) | Lognormal | 12000 | 1200 |
| $T$ (N.mm) | Gumbel | 90000 | 9000 |
| $S_y$ (MPa) | Normal | 220 | 22 |
| $\theta_1$ (rad) | Normal | 0 | $\pi/4$ |
| $\theta_2$ (rad) | Normal | 0 | $\pi/4$ |

**Table 9.** Results of various methods for Example 5

| Method | $\beta$ | $P_f$ | Iterations | G-Evaluations | $\|\beta-\beta_{MCS}\|$ |
|---|---|---|---|---|---|
| *HLRF* | Not convergence | ------------- | ---- | ---- | ------- |
| *iHLRF* | 3.3687 | 0.0003775 | 30 | 972 | 0.4165 |
| *DSTM* | 3.3687 | 0.0003787 | 22 | 264 | 0.4165 |
| *CFSL* | 3.3689 | 0.0003773 | 31 | 372 | 0.4163 |
| *NNCM-Taylor* | 3.3755 | 0.0003682 | 19 | 228 | 0.4097 |
| *NNCM-Pade* | 3.3894 | 0.0003501 | 11 | 143 | 0.3958 |
| *MCS* | 3.7852 | 0.0000767 | ---- | $2\times10^6$ | 0.0000 |

**Table 10.** Probability distribution of random variable for Example 6

| Variable | Distribution | Mean | Standard deviation |
|---|---|---|---|
| $A_1$-$A_6$ (m$^2$) | Normal | 0.013 | 0.0013 |
| $A_7$-$A_{12}$ (m$^2$) | Normal | 0.01 | 0.001 |
| $A_{13}$-$A_{24}$ (m$^2$) | Normal | 0.016 | 0.0016 |
| $E_1$ (KN/ m$^2$) | Normal | $240\times10^6$ | $24\times10^6$ |
| $E_2$ (KN/ m$^2$) | Normal | $220\times10^6$ | $22\times10^6$ |
| $E_3$ (KN/ m$^2$) | Normal | $205\times10^6$ | $20.5\times10^6$ |
| $P_1$ (KN) | Gumbel | 12 | 3 |
| $P_2$- $P_7$ (KN) | Gumbel | 12 | 2.4 |
| $\theta$ (rad) | Normal | 0 | $\pi/6$ |

**Table 11.** Results of various methods for Example 6

| Method | $\beta$ | $P_f$ | Iterations | G-Evaluations | $\|\beta-\beta_{MCS}\|$ |
|---|---|---|---|---|---|
| *HLRF* | Not convergence | ------------- | ---- | ---- | ------- |
| *iHLRF* | Not convergence | ------------- | ---- | ---- | ------- |
| *DSTM* | 3.0706 | 0.000106 | 22 | 1562 | 0.1697 |
| *CFSL* | 3.0706 | 0.000106 | 53 | 3763 | 0.1697 |
| *NNCM-Taylor* | 3.0706 | 0.000106 | 20 | 1420 | 0.1697 |
| *NNCM-Pade* | 3.0706 | 0.000106 | 13 | 950 | 0.1697 |
| *MCS* | 3.2403 | 0.000597 | ---- | $10^6$ | 0.0000 |

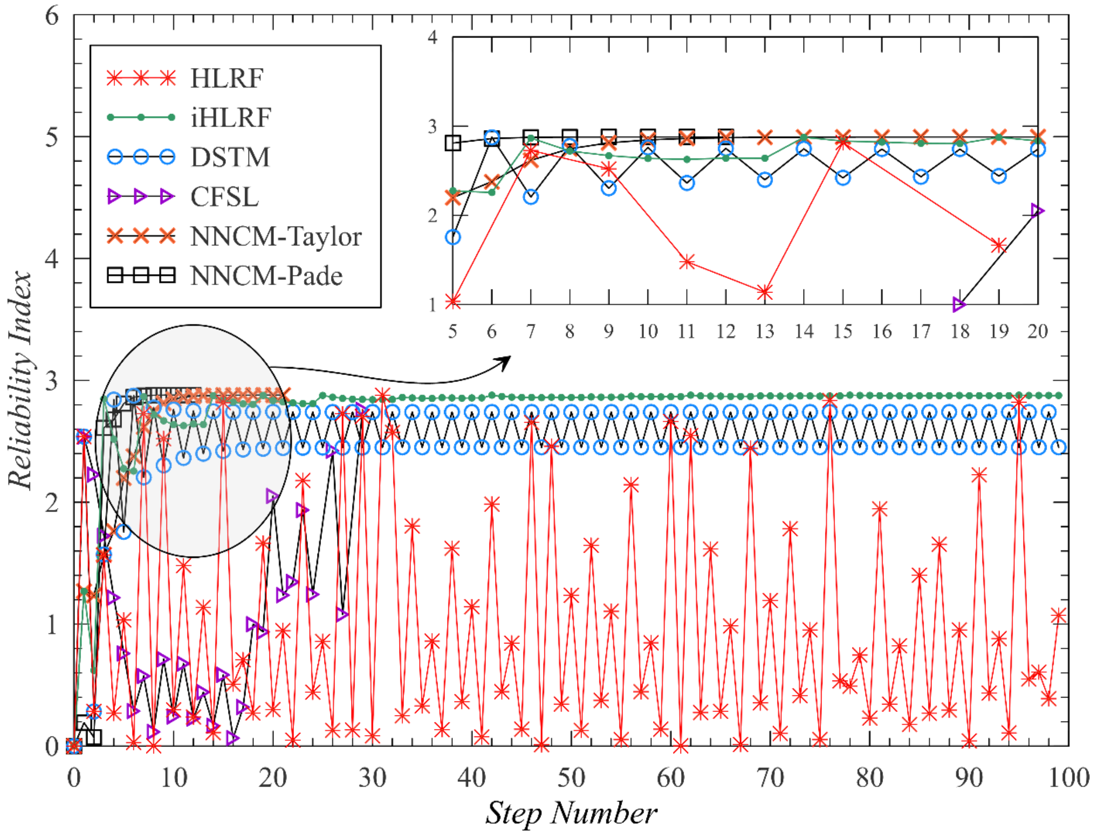


**Fig. 1.** Iteration history for Example 1

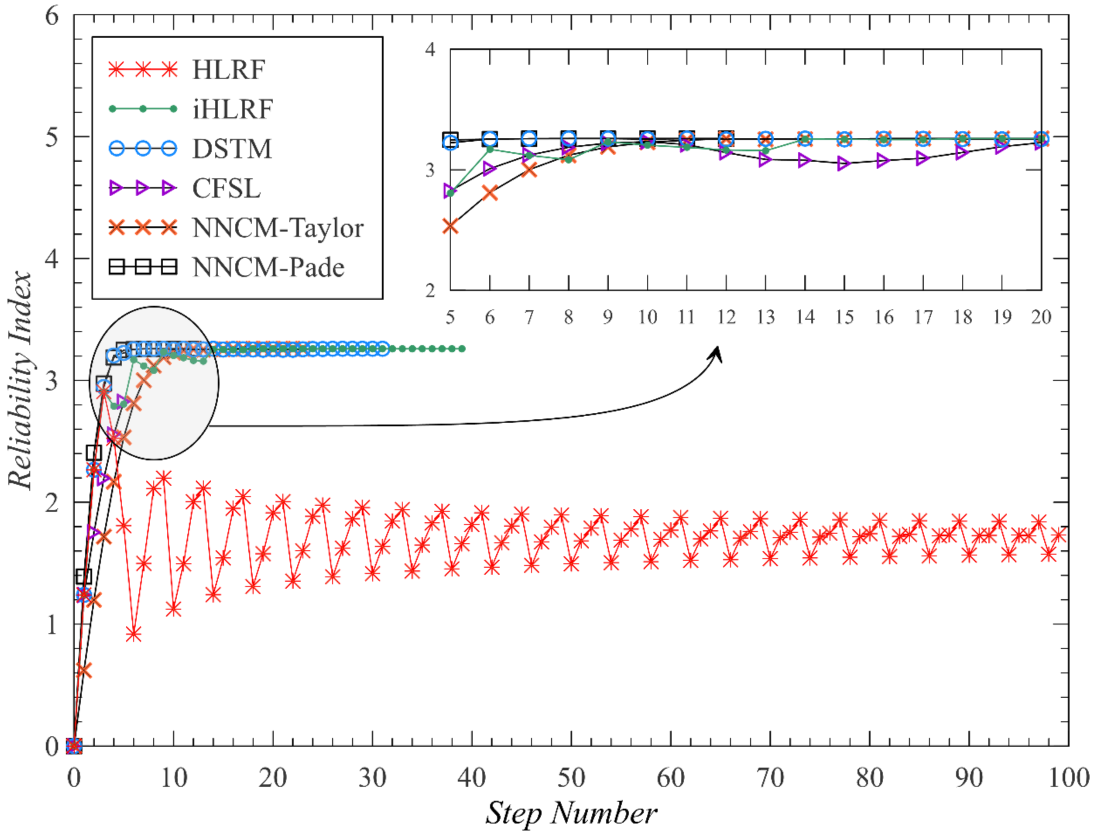


**Fig. 2.** Iteration history for Example 2

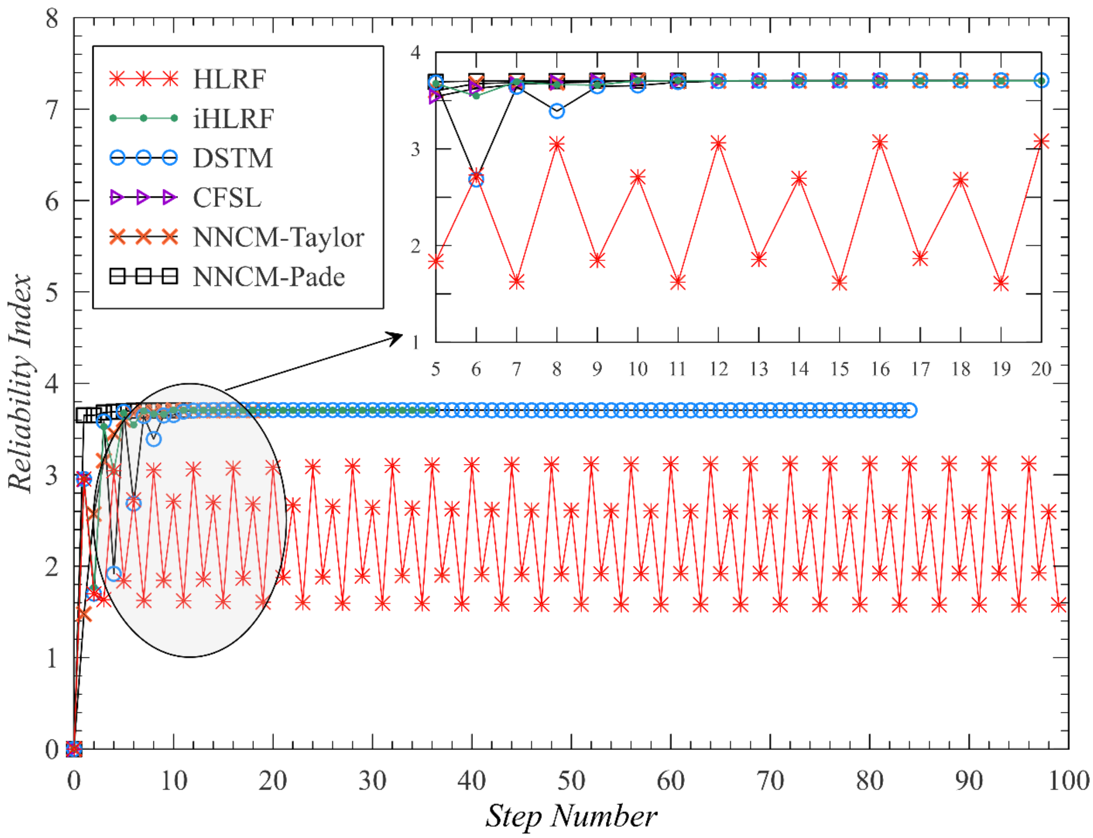


**Fig. 3.** Iteration history for Example 3

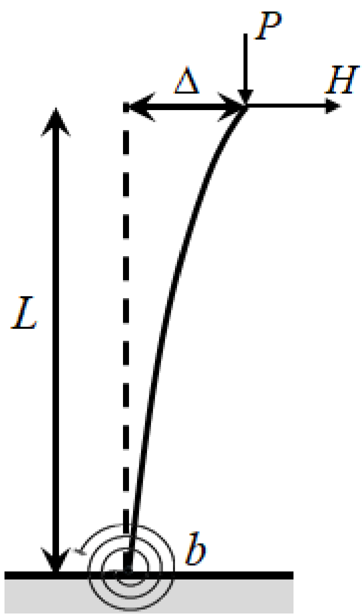


**Fig. 4.** Column of Example 4

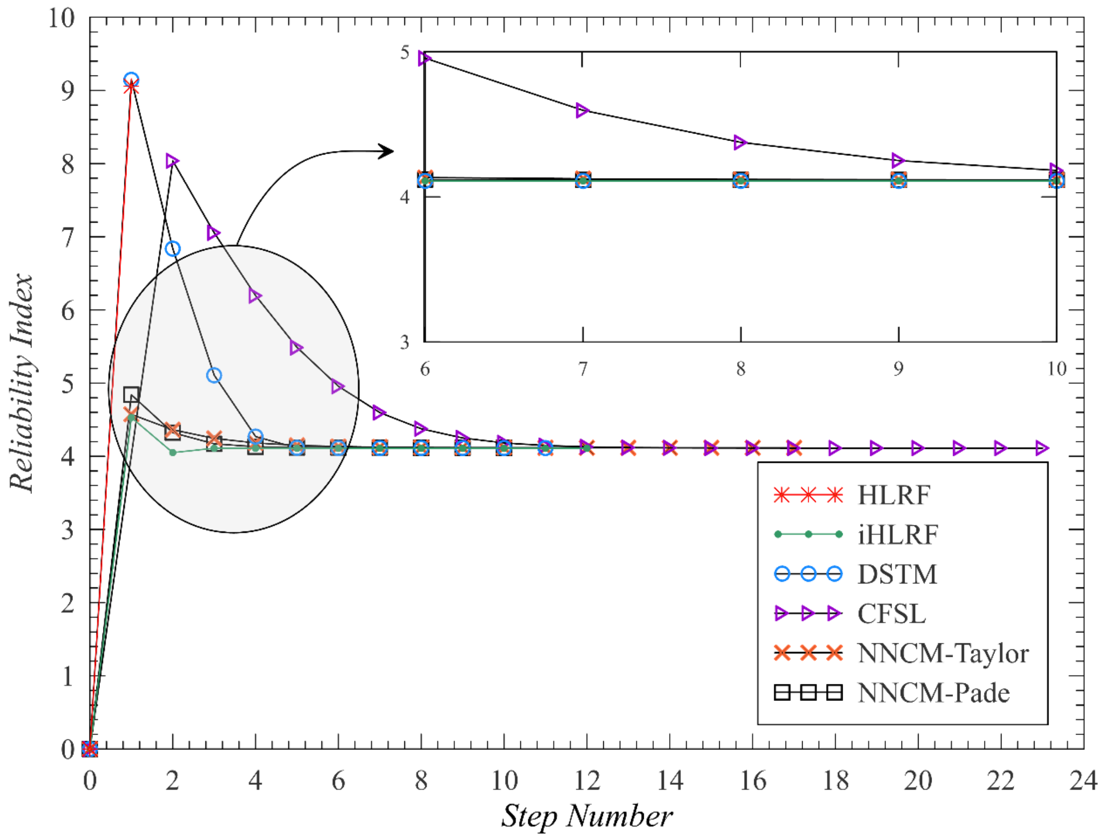


**Fig. 5.** Iteration history for Example 4

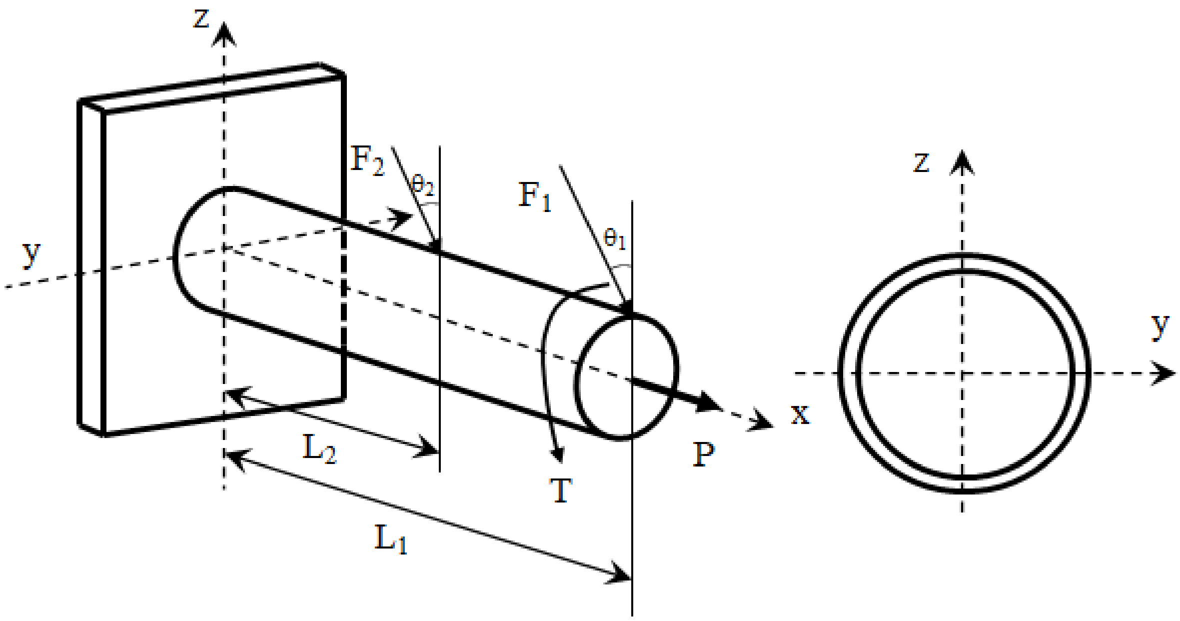


**Fig. 6.** Cantilever tube of Example 5

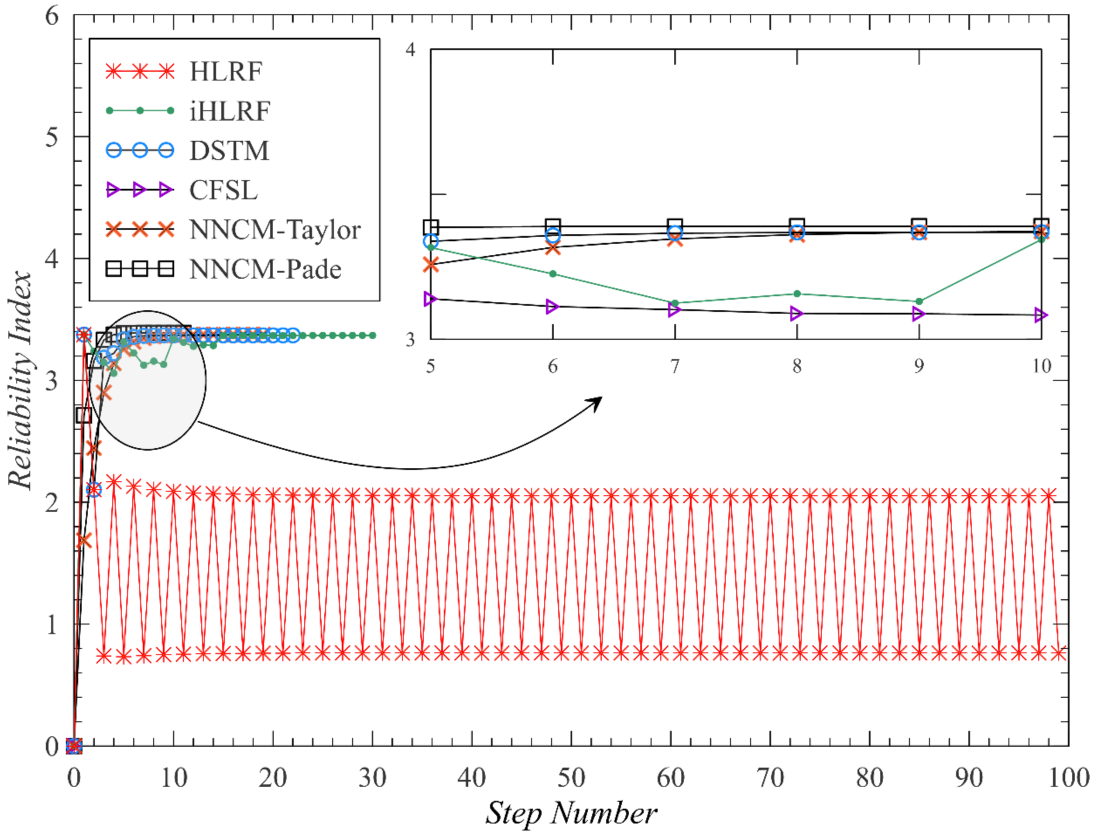


**Fig. 7.** Iteration history for Example 5

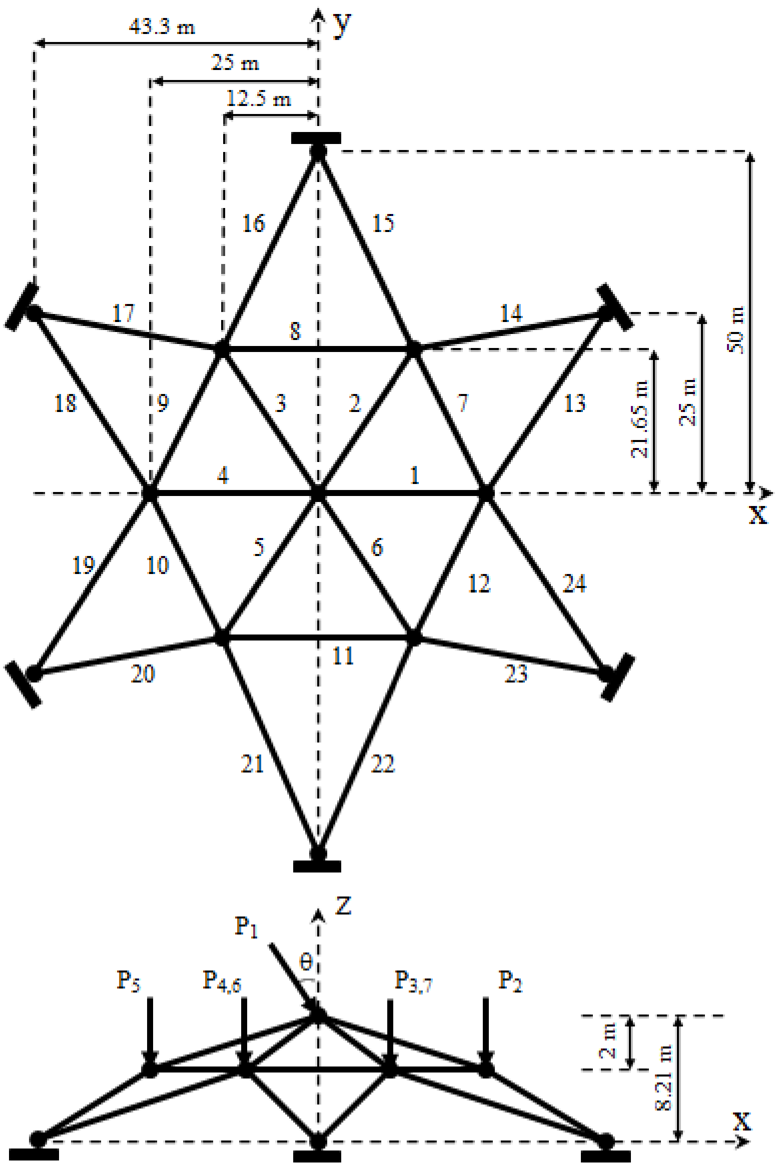


**Fig. 8.** Space truss of Example 6

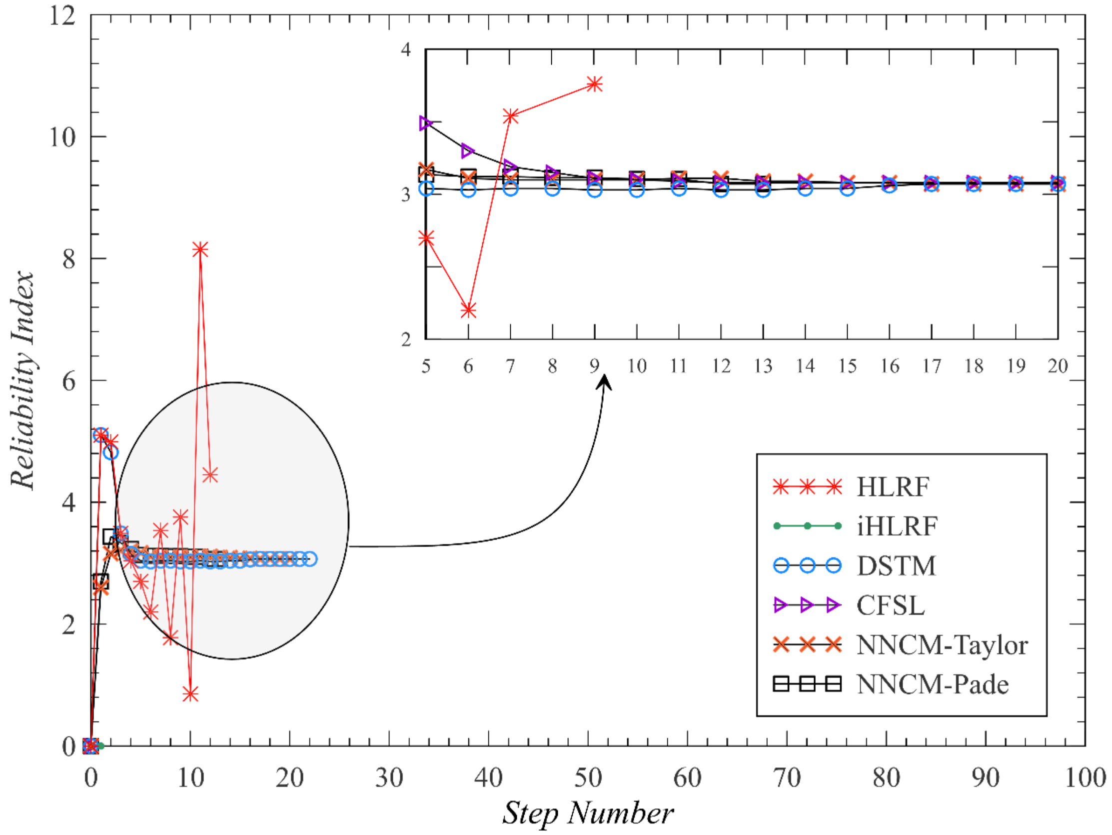


**Fig. 9.** Iteration history for Example 6

## Biographies

**Mehrshad Ghorbanzadeh** was born in March 1989 in Tehran, Iran. He obtained his BSc degree in civil engineering from Zanjan University of Zanjan, Iran. He continued his graduate studies and obtained an MSc degree in structural civil engineering from Shahid Rajaee Teacher Training University of Tehran, Iran. At the moment, he is a PhD student at the Faculty of Engineering, Department of civil Engineering, Kharazmi University of Tehran, Iran. His research interests include reliability analysis, methods and combination of optimization and analysis procedure.

**Peyman Homami** is a faculty member in Civil Engineering department of Kharazmi University, Tehran, Iran. He received his Ph.D. from Tarbiat Modares University in 2008. Dr. Homami's research area includes structural reliability, design and construction of special structures and rehabilitation methods. He has been involved in several national and international infrastructure projects. He has structural design and construction management career.

**Mohsen Shahrouzi** received BS in Civil Engineering and MS in Earthquake Engineering from Sharif University of Technology in 1997 and 2000, respectively. He continued his studies at International Institute of Earthquake Engineering and Seismology until graduated with a PhD degree at 2006. Dr. Shahrouzi is a faculty member in Civil Engineering department of Kharazmi University and has already been the author of over 140 research papers. His research interests include soft computing, graph theory, optimization and reliability analysis in civil engineering and earthquake resistant design of structures.